# iFlyNet: Inferring UAV Flight from Wing Behavior

O. TANAY TOPAC, CODY GRAY, AMRITA KUMAR
and FU-KUO CHANG

## ABSTRACT

We introduce iFlyNet, a novel flight state awareness system that is robust, low-profile, and more reliable in harsh conditions than conventional methods. The system interprets the global flight state of a UAV by monitoring multimodal structural characteristics of its wings, where aerodynamics are predominant. A microfabricated transducer array consisting of temperature compensated strain and piezoelectric sensors captures the wing's static and dynamic stress profiles at multiple spatial locations. This data informs our deep one-dimensional convolutional neural network-based sensor fusion algorithm designed to run on flight vehicle computer at near real-time speeds. Wind tunnel experiments with the sensors installed on a single wing demonstrate that iFlyNet can accurately predict the flight state variables of airspeed and angle of attack across the flight envelope of the UAV. In addition, we also show the benefits of our system compared to status-quo techniques through accurate predictions of lift and drag forces and high-precision tracking of stall occurrence at highly variable environmental conditions. By nearly matching the readings of traditional state measurement devices at a fraction of weight as well as providing accurate predictions of flight performance and safety-critical metrics, our system offers a unique paradigm for aircraft state identification.

## INTRODUCTION

Aerospace engineering has long relied on two fundamental principles: (i) Modeling the physical behavior of aircraft accurately during the development phase, so the manufactured aircraft's behavior aligns closely with the design-phase expectations, and (ii) acquiring flight conditions of aircraft accurately during the operation phase, so the pilot has a robust situational awareness of the aircraft [1]. Conventionally, these two

Tanay Topac, PhD Student, Email: tanaytopac@stanford.edu. Department of Aeronautics and Astronau- tics, Stanford University, Stanford, CA, USA.
Cody Gray, Software Engineer, Email: cody gray@acellent.com. Acellent Technologies, Sunnyvale, CA, USA.
Amrita Kumar, Executive Vice President, Email: akumar@acellent.com. Acellent Technologies, Sunny- vale, CA, USA.
Fu-Kuo Chang, Professor, Email: fkchang@stanford.edu. Department of Aeronautics and Astronautics, Stanford University, Stanford, CA, USA.

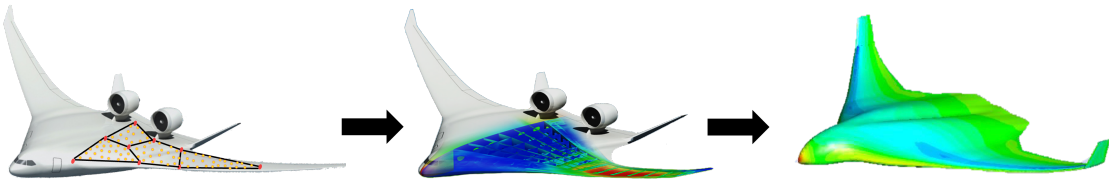

Figure 1. Illustration of the modeling paradigm that the current study is based on. Inspired by avian flight, distributed sensors on wing capture multi-local structural characteristics, which describe the overall structural state of the component. With such a deep knowledge, fluid-structure relations are accurately inferred to estimate the global flight characteristics of aircraft.

principles have largely been decoupled. The former generally concerned the design and analysis engineers while addressing the latter has been the responsibility of avionics and reliability engineers. Nevertheless, recent developments in numerical simulation techniques [2] and accurate data-driven representations achieved by advanced models [3–5] started bringing the aforementioned disciplines closer in the pursuit of developing constantly updating *"digital twin"* models of aircraft from real-time sensor data [6, 7].

The idea of inputting real-time sensor data to a model as its initial/boundary condition(s) is broad and practiced in countless applications. The current study investigates the case in which a number of sensors capture structural mechanics-related data of an aircraft wing, and the model predicts metrics related to global flight characteristics of the aircraft. Fluid-structure interaction research suggests a close coupling between the structural state of an aerodynamic component and the global response of the aerodynamic body and motivates this approach [8]. Moreover, a review of avians' flight routines also reveals that biology also chooses a similar *fly-by-feel* approach, where birds become aware of their flight environment by considering the loading in their wings [9].

Inspired by biological flight, the current study introduces a data-driven modeling technique for interpreting flight aerodynamics of aircraft from distributed multi-modal sensors that capture structural characteristics of one of the wings, as illustrated in Figure 1.

The rest of this article is organized as follows: First, the hardware platform consisting of a sensor network-embedded UAV is introduced. Then, the data acquisition specifications of the sensors, along with the wind tunnel experimentation setup, are discussed. Following hardware, the iFlyNet software is introduced. By detailing the system architecture and estimation models, the working principles of the real-time flight awareness system are laid out in this section. After discussing the methods, a comparison of metrics measured by a set of wind tunnel sensors and estimated via the proposed approach is presented for a representative flight condition. Finally, the article is concluded with remarks.

## HARDWARE SETUP

### Sensor Network-integrated UAV

The system presented in this study is demonstrated on a Blackswift S0 Unmanned Aerial Vehicle (UAV) through wind tunnel experiments. The vehicle, which is originally

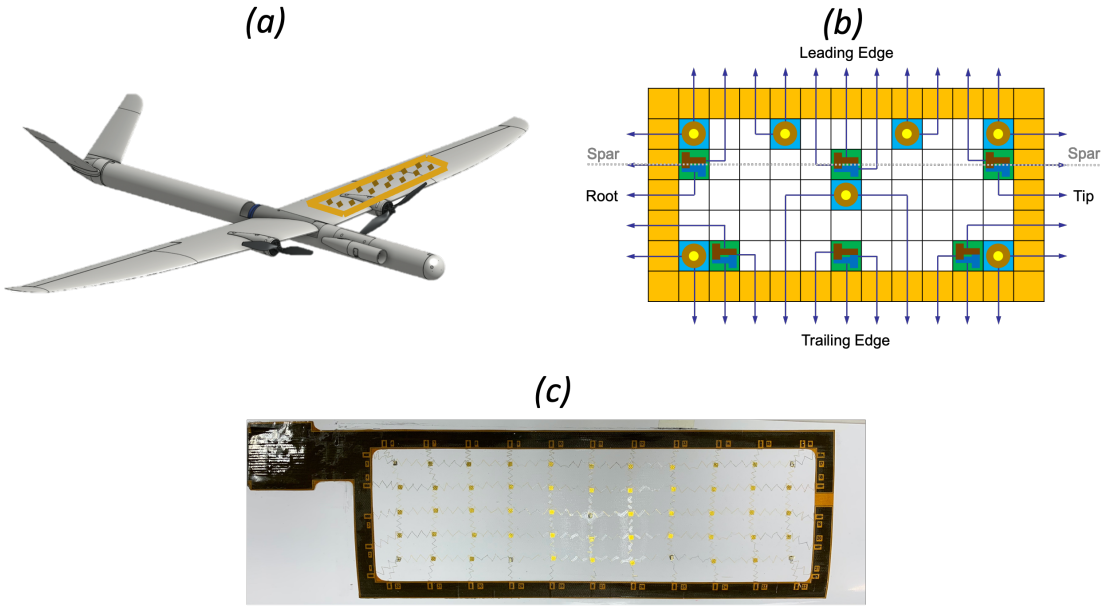


Figure 2. (a) An illustration of the UAV with the sensor network embedded in one of its wings. (b) The sensor network layout. (c) Final wing surface with integrated sensor network after vacuum bagging operation.

designed to make high-resolution atmospheric thermodynamic measurements, contains a rich set of built-in sensors that provide an excellent comparison basis to the proposed system. In addition, its high aspect ratio wing design with 54.6 in. span, closed wingbox structure, and SwiftCore flight management system with persistent telemetry data are several other factors that prompted us to choose this platform.

Distributed multimodal sensing is enabled by a stretchable sensor network deployed to the left wing of this UAV, as illustrated in Figure 2(a). The sensor network consists of 7 PZTs and 6 co-located SG/RTD pairs distributed strategically to maximize the information collected from the wing. By employing SG and RTD elements that share the same spatial locations, an effective compensation mechanism for removing thermal strain effects is achieved. The layout of the sensor network is given in Figure 2(b), and more details on it can be found in [10]. Upon microfabrication and bi-directional stretching, the sensor network is permanently integrated into the wing via vacuum bagging, as shown in Figure 2(c).

**Data Acquisition**

The analog data collected by the sensor network hardware is digitized by the IMGenie Pro Data Acquisition Unit (DAQ) developed by Acellent Technologies. The device, which allows for continuous sampling from all deployed sensors, is designed with sensor network specifications in mind. The most important of these is the utilization of a custom Wheatstone bridge amplification circuit to accommodate the uniquely high resistance values of the SGs and RTDs in the system compared to their commercial counterparts. Introduced due to the very thin profile of the sensors, the devices have a nominal resistance of approximately 15 kOhm as opposed to the common 350 Ohm profile. More details on the sensor network can be found in [10], and more details on IMGenie Pro can

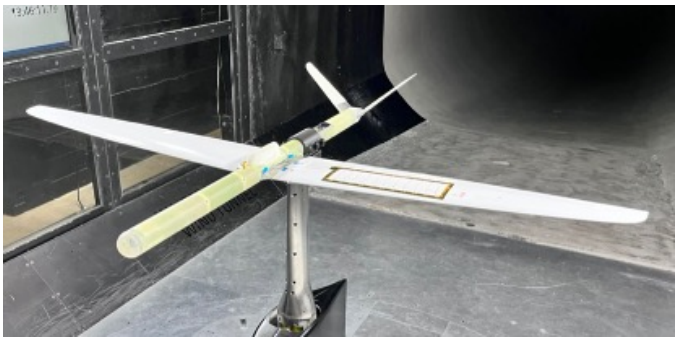

Figure 3. Experimental UAV in the wind tunnel.

be obtained from Acellent Technologies.

The data from PZTs and SGs/RTDs are collected at a fixed resolution of 16-bit and variable sampling rates of 10,000 Hz and 125 Hz, respectively. The 16-bit resolution is confirmed to give greater than 0.1 °C and 1 $\mu\epsilon$ measurement precision, which are deemed adequate for the current application. The variable sampling rate ensured capturing high-frequency dynamics via PZTs while minimizing the power and storage requirements for the static measurements.

**Wind Tunnel Experimental Setup**

A full-scale system test is performed in a closed-throat subsonic wind tunnel of a test section 7 ft. x 10 ft. x 12 ft. (h, w, l). The experimental UAV is placed in the wind tunnel with variable pitch control, as shown in Figure 3. Since the flight vehicle is tested as opposed to an aerodynamic model, precautions such as tightly securing the control surfaces are taken to ensure safe and consistent experimentation. During tests, data is collected simultaneously from (i) built-in wind tunnel sensors, (ii) built-in UAV sensors, (iii) IMGenie Pro, and (iv) five video cameras overlooking the wind tunnel and synchronized in post-processing.

The wind tunnel tests consisted of training data collection and dynamic model evaluation campaigns. In the training campaign, the aircraft is exposed to airspeed and angle of attack combinations that comprise a finely discretized set of its flight envelope (airspeed: [7-20] m/s, AoA: [0-16]°, each with 1 unit increments), as in Figure 4(a). Through this process, a balanced and well-controlled pool of labeled sensor data is collected for training the models. For the dynamic test campaign, on the other hand, the objective has been to collect datasets representative of real-life flight scenarios for inference-time model performance evaluation. Four dynamic campaigns are conducted with the airspeed and angle of attack of the UAV altered semi-randomly within the flight envelope of the UAV. The flight condition sequence for two of the dynamic tests is given in Figure 4 (b).

## SOFTWARE SETUP

**System Architecture**

The iFlyNet flight awareness system involves inferring three key flight metrics of the UAV from sensor network data. These are (i) whether the aircraft is experiencing

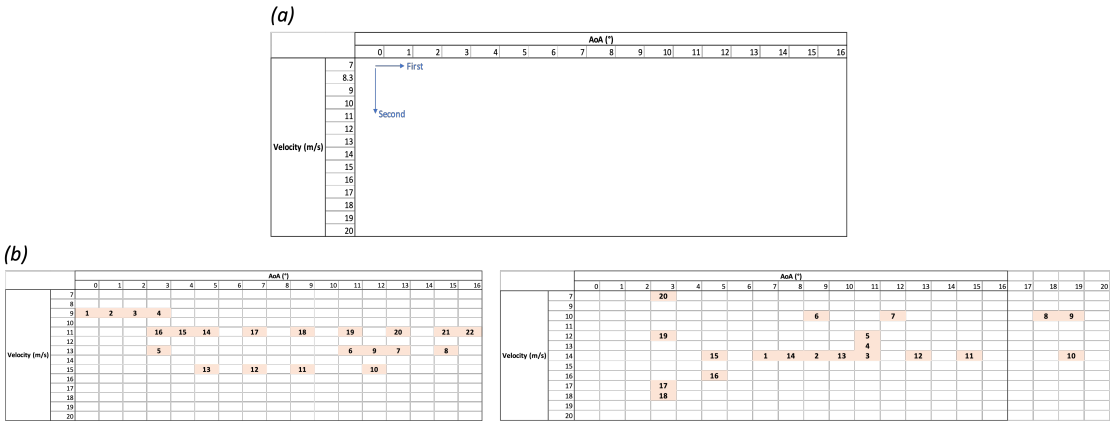


Figure 4. Wind tunnel test campaigns. (a) Model training campaign, (b) dynamic test campaign

stall condition, (ii) airspeed ($V_\infty$) and angle of attack (AoA) variables of the aircraft, and (iii) lift and drag forces exerted on the aircraft. These estimations are made by supervised learning models that continuously run in inference mode to provide near real-time awareness. The model details are discussed in the following section.

The real-time behavior of estimations is achieved by ensuring that the models run at a continuous 30Hz rate, i.e.: A new estimation is made from the most recent data every 0.03 seconds. In accordance with the sampling rates, the inference batches consist of 333 data points for PZT and 4 data points for the SG/RTD. As previously mentioned, this mismatch is introduced to optimize the data fidelity, power consumption, and storage characteristics of the DAQ. For model training purposes, the mismatch is alleviated by extrapolating the SG/RTD data with a linear interpolator. In training time, the entire training and validation set data are inputted into the models in batches. On the other hand, in inference time, the dynamic data is continuously fed to the models, and the models are asked to make estimations at a 30 Hz rate, as described earlier.

**Estimation Models**

In this study, the three key metrics of stall, piloting variables ($V_\infty, AoA$), and aerodynamic performance (lift, drag) are estimated via three distinct neural networks. By decomposing the discrete binary vs. continuous variables (i.e.: stall vs. others) and by grouping similar physics interpretations (i.e.: ($V_\infty$ and AoA) vs. (lift and drag)) this multi-model approach is found to produce greater performance than a single model. In both training and inference tasks, the model inputs consist solely of the PZT and SG data, where all sensors are concatenated to produce synchronized 13-channel data. The outputs, on the other hand, are different for each model, and they are set to the related estimation metric(s) of the corresponding model (stall, ($V_\infty, AoA$) or (lift, drag)).

The wind tunnel data is split threefold into training, validation, and test sets. Training and validation sets consist of the data collected in the *model training campaign* phase of wind tunnel experiments, shown in Figure 4 (a). The specific data that go into the training and validation sets are determined by performing a randomized 90% / 10% split on each flight condition in the training campaign. This process ensured that the training and validation data sets are unbiased in terms of flight condition homogeneity as well as

the timing of the data points. On the other hand, the test dataset contains the $\tilde{7}$-minute continuous data collected in the run #1 of *dynamic test campaign* (Figure 4 (b)). This split is aimed to generate two model performance evaluation bases, one with the static condition data (validation set data) and one with dynamic condition data that represents the actual use case of the system (test set data).

## RESULTS

Among the metrics estimated by iFlyNet, stall is clearly the simplest flight state to identify, as the elevated vibration is a readily observable feature of the stall condition. In the task even a logistic regression gives nearly 90% accuracy on the validation data, a shallow 1-dimensional Convolutional Neural Network (1D-CNN) model of 2 layers with binary cross-entropy loss is found to demonstrate near-perfect performance on both training (99.4%) and validation (99.6%) sets as shown in Figure 5 (a).

Prediction of ($V_\infty, AoA$) and (lift/drag), on the other hand, is much more involved. Different from the stall classification, these tasks are posed as a regression problem to estimate the real-valued number via a mean-squared loss as follows:

$$MSE_{piloting} = \sum_{i=1}^{samples} (V_{\infty,i} - \widehat{V_{\infty,i}})^2 + (AoA_i - \widehat{AoA_i})^2 \tag{1}$$

$$MSE_{aero} = \sum_{i=1}^{samples} (L_i - \widehat{L_i})^2 + (D_i - \widehat{D_i})^2 \tag{2}$$

In these tasks, the aforementioned shallow 1D-CNN architecture is underfitted to the data, presumably due to the few numbers of parameters in the shallow model being unable to model the continuous nature of the estimation task and the rich estimation space effectively. In order to provide greater descriptive power, 1D implementation of the ResNet (1D-ResNet) [11] architecture is employed as the alternative scheme, and the outcomes are significantly improved. Tracking the MSE variables as the performance indicators, the ($V_\infty, AoA$) and (lift, drag) models achieved an aggregated average of 0.07 and 0.02 on the training set, 0.18 and 0.04 on the validation set, and 0.75 and 0.11 on the dynamic test set, respectively, as shown in Figure 5 (a, b). These results suggest near-perfect modeling of the training data while indicating less favorable performance in the dynamic conditions on piloting variables ($V_\infty, AoA$). However, we remark that these figures with less than one unit of aggregated average error in the estimation of piloting variables are still very close to the ground truth measurements.

For visualizing the estimated flight state in comparison with the ground truth measurements a user-facing graphical interface is developed. This user interface, a snapshot of it shown in Figure 6, is developed to run dynamic run campaigns and is composed of three main elements. On the top left, a video stream from a camera overlooking the UAV is displayed. The background of this picture also contains a screen with real-time updating measurements made by built-in wind tunnel sensors. On the top right, a graphic with the estimated state of the UAV is presented. Similar to the measurements, it displays real-time updating estimations of the stall condition and ($V_\infty, AoA$) variables. Finally,

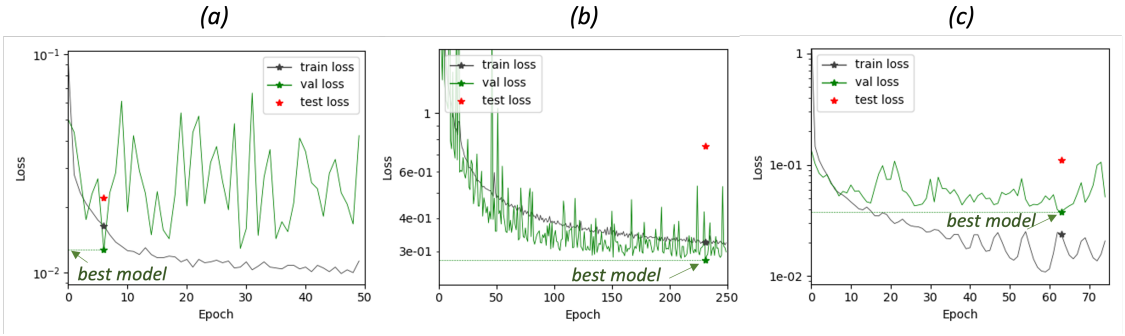


Figure 5. Model performance metrics during training. (a) Stall training, (b) $(V_\infty, AoA)$ training, and (c) (lift/drag) training.

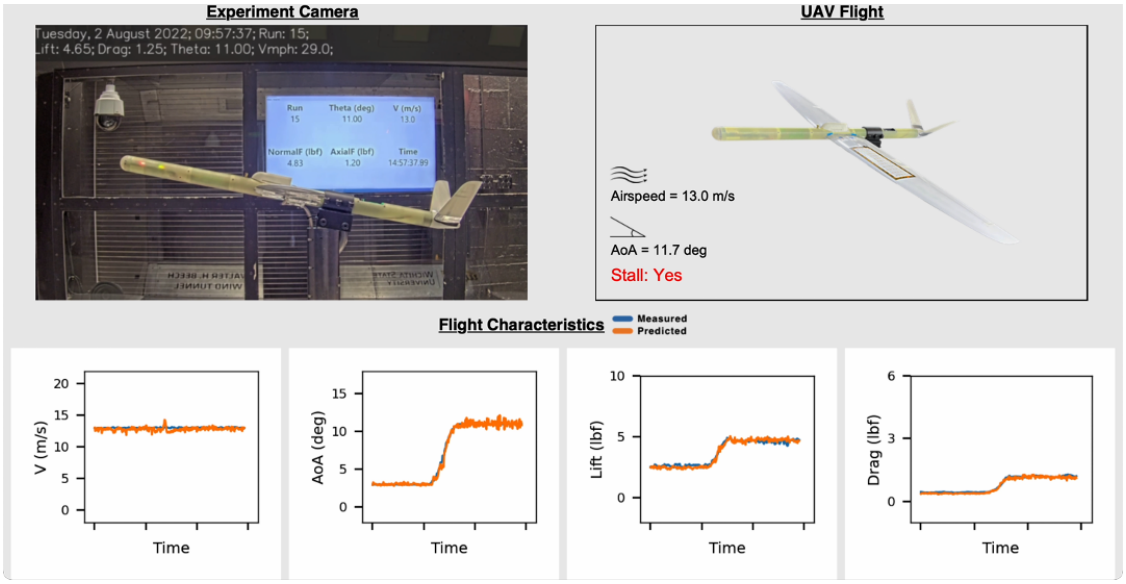


Figure 6. A snapshot from the flight visualization graphical interface.

on the bottom row, four line charts are drawn. These plots show the time history evolution of measured and predicted values of $V_\infty$, AoA, lift, and drag as the wind tunnel experiment progresses.

## CONCLUSIONS

This study presents a modeling approach and a full-scale application example for estimating key flight metrics of aircraft from the mechanical behavior of one of its wings. The technique, inspired by the flight awareness paradigm of avians, hypothesizes that a granular understanding of an aircraft wing's mechanical response can enable inferring global-level flight aerodynamics via a data-driven model. Traditional physics-based techniques are shown to produce such a relationship, however, current work is the first in literature, to our knowledge, that performs this at near real-time speeds and from a physical sensing system.

In the presented application, the technique is demonstrated on a medium-altitude

close-range UAV placed in a subsonic wind tunnel. The combined static and dynamic response that represents the wing's mechanics is collected via a sensor network that distributes a set of PZTs and SGs at strategic locations on one of the wings of this UAV. A family of 1D-CNN-based models is found to provide a high level of estimation performance while satisfying real-time computation speeds. The high accuracy levels obtained illustrate the applicability of the proposed technique as an alternative flight instrumentation paradigm that can improve the safety and efficiency of air vehicles.

## ACKNOWLEDGMENTS

This study is supported by the U.S. Air Force Office of Scientific Research under grant FA9550-19–0213. Support for this study is also provided by U.S. Air Force Research Laboratory under contract FA864921P1617.

## REFERENCES

1. Raymer, D. 2012. *Aircraft Design: A Conceptual Approach, Fifth Edition*, American Institute of Aeronautics and Astronautics, Inc., Washington, DC, ISBN 978-1-60086-911-2, doi:10.2514/4.869112.
2. Hwang, J. T. and J. R. Martins. 2018. "A Computational Architecture for Coupling Heterogeneous Numerical Models and Computing Coupled Derivatives," *ACM Transactions on Mathematical Software*, 44(4):37:1–37:39, ISSN 0098-3500, doi:10.1145/3182393.
3. Topac, O. T., S. Y. Sara Ha, X. Chen, L. Gamble, D. Inman, and F.-K. Chang. 2022. "Hybrid Models for Situational Awareness of an Aerial Vehicle from Multimodal Sensing," *AIAA Journal*:1–10, ISSN 0001-1452, 1533-385X, doi:10.2514/1.J061926.
4. Kopsaftopoulos, F., R. Nardari, Y. H. Li, and F. K. Chang. 2018. "A Stochastic Global Identification Framework for Aerospace Structures Operating under Varying Flight States," *Mech. Syst. Signal Process.*, 98:425–447, ISSN 10961216, doi:10.1016/j.ymssp.2017.05.001.
5. Chen, X., F. Kopsaftopoulos, Q. Wu, H. Ren, and F. K. Chang. 2019. "A Self-Adaptive 1D Convolutional Neural Network for Flight-State Identification," *Sensors (Switzerland)*, 19(2), ISSN 14248220, doi:10.3390/s19020275.
6. Phanden, R. K., P. Sharma, and A. Dubey. 2021. "A Review on Simulation in Digital Twin for Aerospace, Manufacturing and Robotics," *Materials Today: Proceedings*, 38:174–178, ISSN 2214-7853, doi:10.1016/j.matpr.2020.06.446.
7. Aydemir, H., U. Zengin, and U. Durak. "The Digital Twin Paradigm for Aircraft Review and Outlook," in *AIAA Scitech 2020 Forum*, American Institute of Aeronautics and Astronautics, doi:10.2514/6.2020-0553.
8. Dowell, E. H. and K. C. Hall. 2001. "Modeling of Fluid-Structure Interaction," *Annual review of fluid mechanics*, 33:445–490, doi:10.1146/annurev.fluid.33.1.445.
9. Altshuler, D. L., J. W. Bahlman, R. Dakin, A. H. Gaede, B. Goller, D. Lentink, P. S. Segre, and D. A. Skandalis. 2015. "The Biophysics of Bird Flight: Functional Relationships Integrate Aerodynamics, Morphology, Kinematics, Muscles, and Sensors," *Canadian Journal of Zoology*, 93(12):961–975, ISSN 0008-4301, doi:10.1139/cjz-2015-0103.
10. Chen, X. 2021. *Design, Fabrication and Integration of Large-Scale Stretchable Strain Sensor Networks*, Ph.D. thesis, Stanford University.

11. He, K., X. Zhang, S. Ren, and J. Sun. 2016. “Deep Residual Learning for Image Recognition,” in *Proc. IEEE Comput. Soc. Conf. Comput. Vis. Pattern Recognit.*, vol. 2016-Decem, ISBN 978-1-4673-8851-1, pp. 770–778, doi:10.1109/CVPR.2016.90.